

Advanced Laminar Flow Control on a Swept Wing – Useful Crossflow Vortices and Suction

Markus J. Kloker¹

Institut für Aerodynamik und Gasdynamik, Universität Stuttgart, 70174 Stuttgart, Germany

Results of high-order direct numerical simulations are summarized for the evolution of crossflow disturbances in incompressible wing-generic boundary-layers with suction at the wall. The concept of smart suction, an adapted combination of the upstream-flow-deformation (UFD) technique and suction, is presented for laminar flow control. In the UFD technique, relatively tightly spaced, useful crossflow vortices are excited once, grow to nonlinearly large amplitudes due to primary instability, and deform the baseflow thus suppressing otherwise naturally growing, nocent vortices with larger spanwise spacing, and do not cause secondary instability that otherwise rapidly invokes turbulence. They can also be excited repeatedly by specially ordered (groups of) suction orifices, leading to suction with distributed flow deformation (DFD), termed DFD suction. Results for suction panels are shown that have a significantly better performance than the otherwise ideal homogeneous suction at the same suction rate. Pinpoint suction can be used to directly attack secondary instability of nocent crossflow vortices: suction underneath the high-shear layer region causing the secondary instability is found to significantly attenuate secondary instability up to complete suppression, at relatively low suction rates.

Nomenclature

c_q	=	non-dimensional suction rate based on chordwise velocity component U_∞
P	=	average porosity of a suction panel - open-to-closed surface area
(u_k')	=	modal amplitude (y -maximum) of chordwise velocity disturbance with wavenumber $k\gamma_0$
v_c	=	maximum suction velocity over a suction orifice, based on U_∞
v_m	=	average suction velocity over a suction orifice, based on U_∞
φ_∞	=	sweep angle of infinite wing or plate
(h,k)	=	disturbance mode designation, frequency $h\omega_0$, spanwise wavenumber $k\gamma_0$

I. Introduction

The substantially grown costs for fuel nowadays can amount up to 40% of the direct operating costs of a long-distance flight. So even before environmental protection laws enforce a decrease in exhaust gases there is vital interest in lowering fuel consumption by lowering the aerodynamic drag of airliners. As the viscous drag share during cruise is about 50% its reduction offers the largest potential for fuel savings. This can be achieved with hybrid laminar flow control (HLFC) by boundary-layer suction on the wings, tail planes, and nacelles with a fuel saving potential of about 16% if laminar flow could be kept up to 40% chord of the respective surfaces. The management of turbulent flow on the aircraft's fuselage - causing about 22% of total drag - by a kind of shark-skin surface structure has a much lower total saving potential, of about 1-2%.

Boundary-layer suction has been known for long to significantly decrease primary laminar instability and thus to push laminar-turbulent transition downstream. In case of swept aerodynamic surfaces with three-dimensional boundary layers suction aims primarily at reducing the inherent, nocent crossflow within the boundary layer by sucking fluid from the outer region of the boundary layer with higher momentum to the wall. The crossflow causes a primary instability of the boundary layer, leading to co-rotating longitudinal vortices, called crossflow vortices (CFVs), that typically trigger a high-frequency secondary instability invoking the substantially drag-increasing turbulent boundary-layer state¹. Distributed discrete suction through a perforated wall in a three-dimensional

¹ Senior Research Scientist and Lecturer, Aerospace Engineering Department, IAG, Pfaffenwaldring 21, 70569 Stuttgart, Member AIAA.

boundary layer can, even in case of a flat surface and unlike the two-dimensional case, excite exponentially growing crossflow modes leading to nocent vortices^{2,3}. Even if a regular spanwise/streamwise hole spacing were applied that is lower than the smallest spanwise/streamwise wavelength of amplified instability modes and thus nominally only the wave numbers corresponding to the spacing and higher harmonics are excited, slight imperfections of the hole order would lead to excitation of amplified lower wave-number modes. There are two ways to smartly arrange the perforations, that preferably are spanwise (finite) slots that cause less amplitudes of three-dimensional modes: (i) the order is gained by an optimization procedure imposing a minimum in the excited streamwise/spanwise wave-number spectrum at the eigenmode combinations², or (ii) the order is such that it deliberately excites useful crossflow vortices that lie closer together than the ones most amplified and thus nonlinearly suppress the growth of other disturbances^{1,4}. The latter technique – smart suction – is based on the upstream-flow-deformation (UFD) technique^{1,5}, shown to work without suction. It is termed UFD suction if one vortex-set is used and excited more than once, and distributed-flow-deformation (DFD) suction if different vortex-sets are used. The method has the advantage that any crossflow disturbances, not only the ones generated by the perforation pattern, can be suppressed.

Instead of decreasing primary crossflow instability or seeding useful vortices by suction it may be instrumental to directly control secondary, or bi-global, instability of the appearing vortices. In other words, the (spatially localized) instability in a two-dimensional plane, here the flow crosscut perpendicular to the vortex core, can be attacked. This can be even useful with deliberately excited vortices, whose nonlinearly large amplitudes vary downstream with varying baseflow, to directly control their stability and thus to secure or enlarge their range of usefulness. The aim is then to prevent or weaken the localized instability of vortex-deformed flow. To this end, localized, pinpoint suction is applied directly underneath the possibly dangerous, localized shear layers invoked by a (crossflow) vortex that transports low-momentum fluid from the wall to the boundary-layer edge inducing spanwise shear $\partial u/\partial z$ (wall-normal vorticity) and wall-normal shear $\partial w/\partial y$, $\partial u/\partial y$ (streamwise, spanwise vorticity). The idea to test this localized suction was fostered by the finding that even a small velocity component normal to a local shear layer can substantially reduce the shear-layer instability^{6,7}.

The high-frequency secondary instabilities of crossflow vortices (CFVs) has been fully elucidated in the last few years experimentally⁸, theoretically⁹, and by means of spatial DNS^{1,6,10}, see also the overview Ref. 5. Recent quantitative comparisons⁶ showed significant deviations between amplification rates from DNS and SLST. The diversity could be traced back to a sensitivity of secondary growth rates with respect to very small changes in the employed two-dimensional primary state, caused by ambiguous simplifying representations of the same deformed primary flow field taken from the DNS. Thus the secondary instability mechanisms seemed to be sensitive to moderate suction or blowing at the wall, providing a good chance to delay transition to turbulence. By means of spatial DNS we show that the amplitude growth rates of artificially excited unsteady high-frequency secondary instabilities can indeed be reduced significantly by exploiting the shear-layer sensitivity with respect to a normal velocity component.

II. Numerical Method

Our proven incompressible DNS code N3D solves the full 3-d unsteady incompressible Navier-Stokes equations in vorticity-velocity formulation in a rectangular domain on a flat plate using a disturbance formulation, where each flow quantity q is divided into its steady baseflow part q_B and its unsteady component q' to ease formulation of the boundary-conditions. All variables are non-dimensionalized using a reference length L and the chordwise freestream velocity U_∞ unless otherwise noted. For the chordwise and wall-normal directions x and y sixth-order compact finite differences are implemented whereas for the spanwise direction z we use a Fourier spectral representation with $K+1$ fully complex modes and the mode counter k , $k=0-K$. Localized suction is considered a disturbance, thus we prescribe a vanishing wall-normal derivative of the wall-normal disturbance velocity component $v'(k=0)$ at the upper edge of the domain outside the boundary layer, where for $v'(k \neq 0)$ an exponential decay is enforced, and we prescribe this component at the wall with the other velocity components zero to locally simulate suction. The basic suction function is $v'_{suc} = v_c(\cos^3(\pi r/d))$ for holes or the chordwise extent of slits and slots, where slots have similar, small local lateral endings; r is the radial coordinate for a hole, d its diameter, and v_c the maximum suction velocity. The average suction velocity over a hole is $0.22v_c$, over a slot approximately $0.42v_c$, or equivalently, the effective diameter of a hole with a v_c -top-hat profile is $0.47d$. Sketches of the integration domain are shown in Fig. 1, and for a detailed description of the numerical method see Refs. 1 and 3. For crossflow suction cases, the method has been verified by comparison with results by Spalart¹¹ that will be shown in an upcoming paper. The DNS are costly, and the NEC SX-8 at the Stuttgart super computing center HLRS has been used.

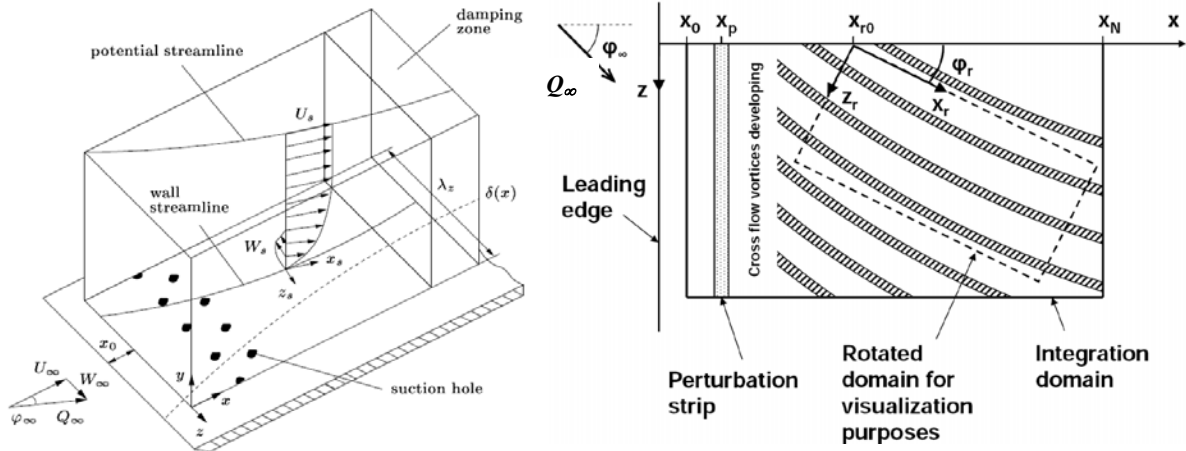


Figure 1. Integration domain. Perspective view (left) and top view (right) on flat plate with vortices, plate-fixed and rotated reference system. The perturbation strip is used for test disturbances.

III. UFD Suction

A. Baseflow

The baseflow considered is the flow on the A320 vertical fin as available from the open EUROTRANS project. The freestream velocity is $Q_\infty=240\text{m/s}$, the sweep angle 40° resulting in the chordwise component $U_\infty=183.9\text{m/s}$, the kinematic viscosity is $\nu_\infty=3.47\times 10^{-5}\text{m}^2/\text{s}$, and the reference length is $L=4\times 10^{-4}\text{m}$. The integration domain in the example shown begins at $x=70$ and ends at $x_N=500$, covering a length of 17.2cm on the fin. The shape factor is $H_{12}=2.32$ at the inflow boundary and weakly rises up to $H_{12}=2.41$ at $x\approx 160$ from where it keeps almost constant. The local Hartree parameter of a virtual Falker-Skan-Cooke flow would be roughly $\beta_H\approx 0.4$ at the inflow boundary and approximately 0.2 for $x>160$. The angle of the potential streamline decreases from $\varphi_e(x_0)=46^\circ$ to $\varphi_e(x_N)=37^\circ$, and the displacement thickness is $1.44\times 10^{-4}\text{m}$ at $x=200$. The maximum crossflow component reaches its maximum of about 9.3% of the local edge velocity u_s at the inflow and continuously reduces to 6.1% at the outflow⁴.

B. Instability Considerations and Results

From a stability analysis for steady crossflow modes we find the band of amplified spanwise wavelengths λ_z to range from $800\text{-}4740\mu\text{m}$ at $x=70$ and from $1850\text{-}19330\mu\text{m}$ at $x=500$, see Fig. 2. The value of the locally most amplified mode increases almost by a factor of 2.5 from $1480\mu\text{m}$ to $3590\mu\text{m}$. For a control strategy based on the principle of the UFD technique this significant shift in the amplified wave-number range implies that a single excitation of UFD-vortices that have about $2/3$ the wavelength of the most amplified mode only can successfully be applied on a short downstream distance. A UFD-vortex excited in the upstream flow region can only stabilize if and as long as its amplitude is large, and since the range of amplified disturbances shifts to larger wavelengths the UFD vortex is damped (in the new meanflow it generates), losing its stabilizing influence. The vortex itself modifies the meanflow but from the original stability characteristics of the underlying baseflow it can already be seen, with sufficient accuracy, when it is damped.

The main idea of our approach is to combine two LFC techniques that have already proven to delay transition in free-flight tests and experiments, namely boundary-layer suction^{11,12} and UFD^{1,13}. The suction orifices serve as excitation sources and are ordered such that useful, closely-spaced (UFD) vortices are generated and maintained on a beneficial amplitude level. ‘‘Maintained’’ means here that the vortex is not incidentally cancelled by anti-phased disturbance input, rather it is supported. Since amplification lacks further downstream, discrete continued excitation helps to keep a level that is limited by the local suction velocity, causing a vortex amplitude typically smaller than the one needed. Indeed we found no significant lift-up effect providing a growing amplitude without discrete modal instability. The issue of keeping up useful vortices is further discussed in the paragraph on DFD suction.

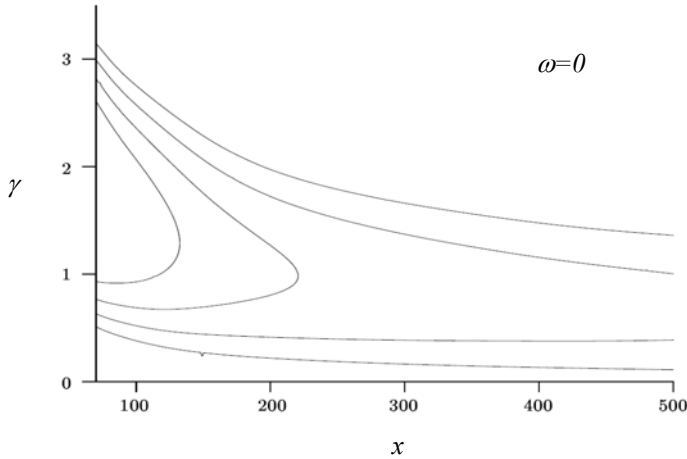


Figure 2. Stability diagram for steady crossflow modes. Isolines of spatial amplification rate $-\alpha_i$, starting with $\alpha_i=0$ (outermost lines) and $\Delta\alpha_i=-0.01$; EUROTRANS baseflow.

$v_c=2.8\%$. The integration domain contains four regularly positioned slots in spanwise direction spaced at $s_z=1570\mu m$, exciting vortices with a spanwise wavenumber $\gamma=1.6$ to suppress the test mode $\gamma=0.8$ considered most dangerous because it is integrally most amplified. Not only the spanwise spacing but also the spanwise position of the slots was kept, and the streamwise spacing, initially $s_x=2200\mu m$ for the first five rows, was adapted to the growing streamwise wavelength of the mode gained at first from the stability analysis of the unaltered baseflow. For further optimization the meanflow altered by the vortices can be extracted from the DNS for the stability analysis, or it can be directly taken from the DNS. (We note that for the different method of minimum modal disturbance input introduced in Ref. 2 it is essential to have corrected values for wavenumbers and receptivity functions for the nonlinearly altered flow by the mean suction effect itself, i.e. the two-dimensional component of the suction disturbance.) Fig. 3 shows the modal amplitude development of the chordwise velocity disturbance u' , exhibiting a maximum of 19% at $x=260$ for the excited and supported mode $\gamma=1.6$. The mean flow distortion, $\gamma=0$, generated by the vortex, increases the pure suction effect of the slots as can be seen by the comparison with the curve for homogeneous suction with identical suction rate. The distance between the two lower curves for the test mode manifests the benefit: For smart suction, the test-mode amplitude is eventually only one fifth the homogeneous-suction value. Of course, this value is lower than without suction (not shown).

Imposing crossflow vortices is a delicate procedure as the danger of triggering turbulence by secondary instability is always present. Time-periodic pulses consisting of 10 frequencies with fixed phase relation have been introduced at $x=185$ at the wall by timewise periodic blowing and suction to check this issue (see Fig. 3, unsteady modes). No secondary instability was found, proving the usefulness of the methodology. Fig. 4a shows on the left a visualization of the vortices in the flow field, and on the right the suction-slot panel.

Fig. 4b illustrates an improper design of the panel. At about one-quarter of the chordwise domain extent the spanwise and streamwise spacing of the slots is increased in a discrete step by 33% to excite the mode $\gamma=1.2$ to adapt to the reducing unstable wavenumbers; additionally a small spanwise shift for every third row has been implemented incidentally. The design fails as the unsteady pulse disturbance is amplified invoking turbulence. The order switch is too early, and a more detailed analysis reveals that nonlinear interactions between both excited ‘‘UFD’’ vortices $\gamma=1.6$ ($k=4$) and $\gamma=1.2$ ($k=3$) lead to destructive nonlinear interference triggering secondary instability in the vicinity of the slot-spacing alteration. The case also proves that secondary instability can set in *on the active suction panel* that imposes a significant negative wall-normal velocity component throughout the boundary layer. This component can alter the secondary instability properties considerably⁶ as discussed in chapter I. We found secondary instability also in cases with constant subcritical hole spacing over the whole panel where however every fourth hole in a spanwise row was regularly misplaced by $0.1s_z$ to mimic a production flow. By contrast, some experimental evidence of working LFC with distributed suction by holes in three-dimensional flows lead to the practical conclusion that the panel ‘‘sucks everything’’, even secondary instability and (early) turbulence.

We note that not destroying the amplitude level by continued discrete suction is not a trivial task because it is not clear a priori which direction the vortices follow – the flow direction depends on the wall-normal distance –, and improper excitation can lead to destructive nonlinear interaction with useful vortices from upstream, or nocent vortices.

A successful example of the method is shown in Figs. 3 and 4a. Slots with a chordwise extent $d_{SL}=160\mu m$ and a spanwise extent of $l_{SL}=890\mu m$ were arranged within $90 \leq x \leq 513$, producing a porosity $P=4.2\%$. The overall suction rate is $c_q=P \times v_m/U_\infty=0.0005$, with an average suction velocity within the slots $v_m/U_\infty=1.2\%$, caused by

To be true, the pure suction effect, $\gamma=0$, would have to be so large that it completely suppressed any modes being able to cause secondary or bi- or tri-global instability despite their higher excitation.

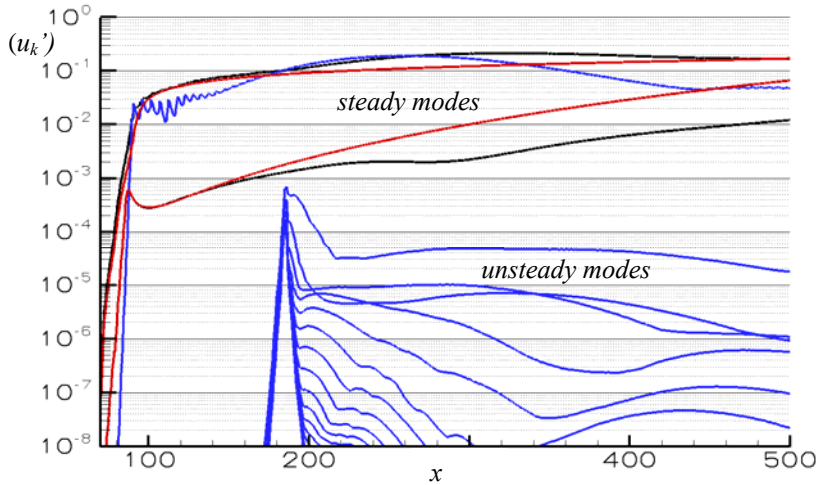


Figure 3. Amplitude development for smart UFD suction with a slot panel. Steady modes: — homogeneous suction, — UFD slot suction, $\gamma=0$ upper, $\gamma=0.8$ (test mode) lower curve in either case; — UFD slot suction, “UFD” mode $\gamma=1.6$. Unsteady modes: pulse disturbances ($\omega=0.45-4.5$, time-spectral) to check for secondary instability.

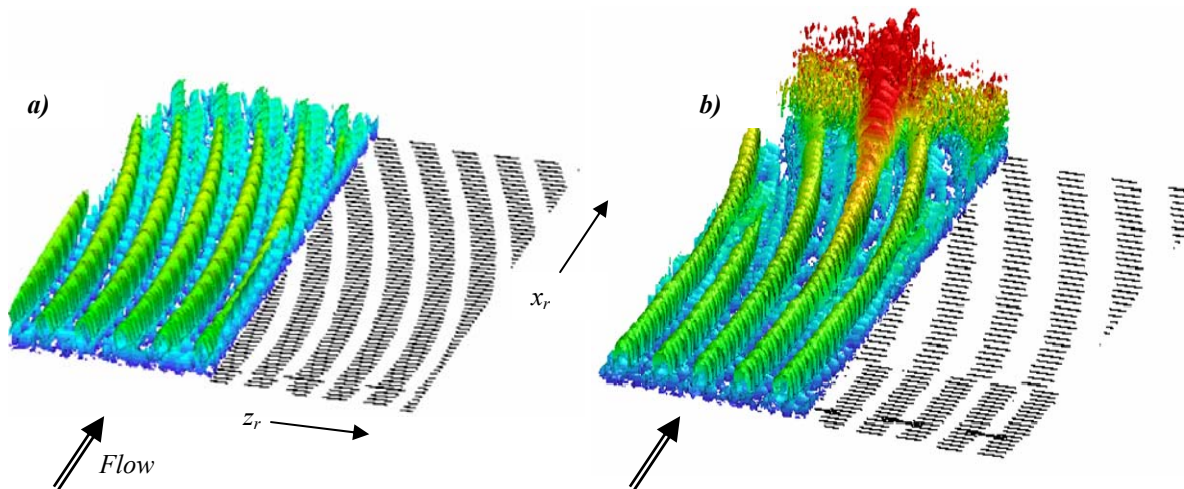


Figure 4. Visualization of vortex structures induced by slot-array suction. Shown are λ_2 iso-contours, the color indicating the wall-normal distance. The underlying micro-slot panel is displayed in grey. Note the compression of the x_r axis. a) stable, smart UFD suction, see also Fig. 3, b) improper (DFD-suction) design, vortices cause secondary instability (red, snapshot). 125% of the spanwise domain width is shown.

The case of Fig. 4b rises the question whether the switch over to another, different stabilizing vortex mode is possible on the panel. This leads to proper DFD suction.

IV. DFD Suction

A. Baseflow

The baseflow of the previous chapter has been modified by a stronger acceleration of the flow (factor 1.7 up to $x=300$) to have a stronger instability alteration within a domain manageable by the DNS. The maximum amplification near $x=100$ now is for $\gamma=2.4$. Moreover, a local baseflow disturbance by a pressure increase has been incorporated to check for sensitivity of the design. Locally, the flow is near laminar separation with $\beta_H \approx -0.195$.

B. General Considerations and Results

If the instability characteristics of the baseflow alter considerably downstream, an adaptation of the stabilizing mode is necessary. In order to avoid destructive nonlinear interference among excited modes leading to dangerous situations with unequally strong vortices as seen above and also as investigated in Ref. 1 without suction, only subharmonic modes are appropriate. The quadratic nonlinearity inherent in the governing equations leads to generation of combination modes $\gamma = \gamma_1 \pm \gamma_2$ and, if $(\gamma_2/\gamma_1) \neq 0.5$, dangerous, possibly amplified modes with $\gamma < (\gamma_1, \gamma_2)$ arise. (Modes with negative values of γ are identical to positive modes for the steady case.) In the case of chapter III $k=4$ and $k=3$ generated not only $k=7$ but also $k=1$, $\gamma=0.4$, leading to unfavorable vortex disorder in the switching region and thus secondary instability. With subharmonic switching, only $k=2, 4, 6, \dots$ emerge, where the higher harmonics are always needed to form a vortex¹.

Figures 5 and 6 present the results of a DFD-suction example using slots where s_x and s_z have been doubled suddenly. The first panel has $c_q = P \times v_m / U_\infty = 0.00082$, with P about 6%, and $v_c = 3.8\%$; the values for the second panel are $c_q = 0.00028$, $P \approx 1.4\%$, and $v_c = 5.0\%$. Six distinct vortices, corresponding roughly to the periodicity length, are visible in Fig. 5a, displaying the reference case without baseflow disturbance. The black dashes indicate the suction slots at the wall. After the switchover it takes $\Delta x_r = 160$ until a distinct three-vortices pattern has evolved. Three out of the six vortices from upstream smoothly fade out. The basic crossflow is from bottom to top, and one vortex of the contra-rotating vortex pair induced by each suction orifice dies out because it tries to transport fluid against the crossflow near the wall locally. Thus only the vortices slightly left of the slots, i.e. at lower z_r values, form to crossflow vortices as seen for $x_r > 360$. For $100 < x_r < 200$ the slot order plays a minor role since the vortices are large and the support or destruction by the slot suction is irrelevant. Figure 5b shows an intermediate phase shift forced by the baseflow disturbance. Compared to Fig. 5a, where every other DFD vortex on the first panel seems to turn into a DFD vortex on the second panel, the DFD vortices now originate from vortices of the first panel that are shifted by one. The baseflow disturbance seems to support the vortex shift by weakening the first vortex pattern. Note that here crossover- w_s -profiles exist. No harm is exerted by the baseflow disturbance on the DFD strategy so far.

Fig. 6 draws the modal amplitude development of the streamwise velocity disturbance $\tilde{u}_s' = u_s' / u_{s,e}$. The first DFD mode is denoted by $(0,6)$, corresponding to $\gamma = 3.0$ in the used frequency $(h\omega_0)$ - spanwise wavenumber $(k\gamma_0)$ spectrum, and the second is $(0,3)$, $\gamma = 1.5$; the test mode $(0,2)$ now has $\gamma = 1.0$. Most importantly, again periodic pulses consisting of $h=1-20$, $\omega_0 = 0.225$, have been added to check for laminar stability. Neither the shift to a lower wavenumber DFD mode nor the baseflow disturbance cause secondary instability.

V. Pinpoint Suction to Control Secondary Instability

A. Basic Setup

We use the baseflow corresponding to the DLR-Göttingen experiment, see Ref. 6, where a flat-plate flow with negative streamwise pressure gradient was generated by a displacement body above. For all simulations $Q_\infty = 19\text{m/s}$ and $\varphi_\infty = 42.5$ holds, thus $U_\infty = 14\text{m/s}$ and $L = 0.1\text{m}$, with $\text{Re}_L = 92000$. Steady crossflow vortices have been triggered⁶, and are subject of secondary-instability control by suction. The integration domain length is $(x_N - x_0) = 0.219\text{m}$ (1674 points) and $y_M = 0.014\text{m}$ (225 points with decreasing step size to the wall); the fundamental spanwise wavelength is $\lambda_z = 0.012\text{m}$ and $K = 13$, $\omega_0 = 6$ (133Hz).

At $x = 3.0$ timewise periodic pulses composed of low-amplitude disturbances with $h = 1-50$ and $k = \pm 1$ are introduced by localized blowing and suction within a disturbance strip at the wall, cf. Fig. 7c. High-frequency modes achieve both the highest amplitudes and the highest growth rates for $x > 3.4$ in the reference case without suction. A more detailed investigation of mode $\omega = 132$ reveals that the corresponding amplitude distribution shows the typical S-shaped type-I mode as visible in Fig. 7a. In the scenario here this mode is known to be responsible for transition to turbulence by generating secondary finger-like vortical structures at the left, updraft side of the vortex.

Suction with $v_c = 10\%$ (based on U_∞ , 7% based on local edge velocity $U_{s,e}$) has been applied within a rectangular orifice situated directly under the position of the amplitude maximum of the secondary mode of one vortex, see Fig 7a. The suction is centered at $x = 3.38$, $z = 0.06$, with dimensions 0.03×0.02 (wherein $-v' > 2\%$), corresponding to $3\delta_l \times 4.5\delta_l$ there. The suction rate is $c_q = 0.0002$ that however depends on the definition of the streamwise extent of the “panel” consisting here of one spanwise hole row, and $s_x = 4.5 - 3.38 = 1.12$. With halved orifice area halving c_q , and optimized position, the results shown below are similar.

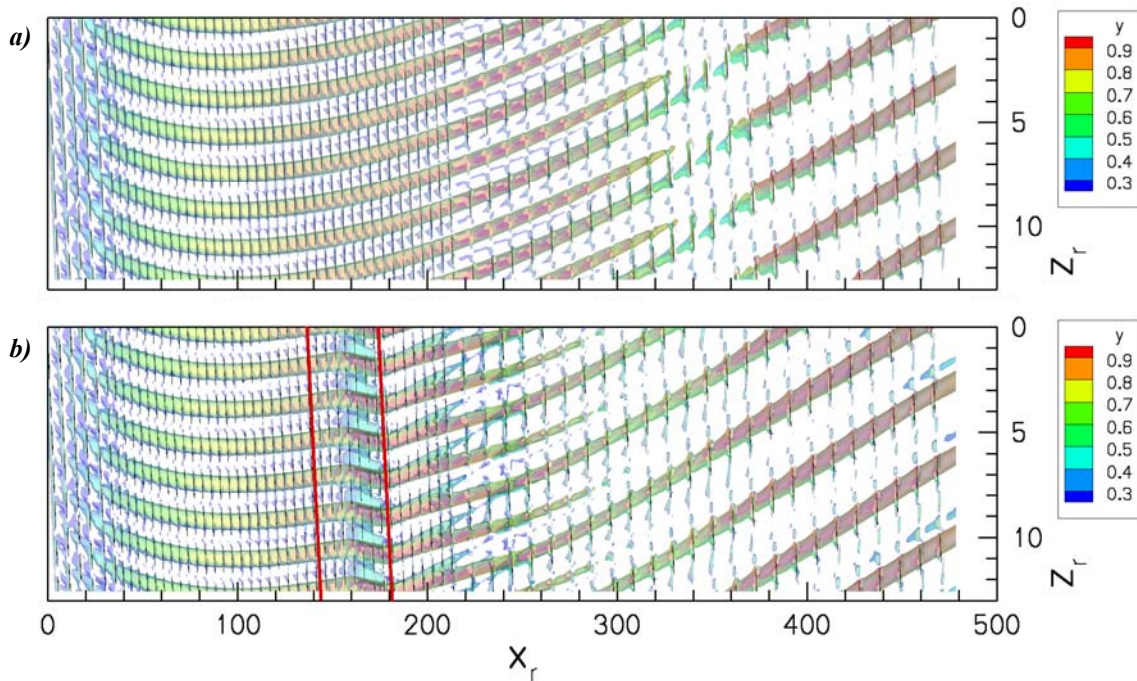


Figure 5. Visualization of vortex structures induced by DFD suction with two slot panels. Shown are λ_2 iso-contours, the color indicating the wall-normal distance. The underlying micro-slot panel is displayed in grey. Note the compression of the x_r axis. a) without baseflow disturbance, b) baseflow disturbed by localized pressure rise between red lines. Top view on plate, mean flow from left to right.

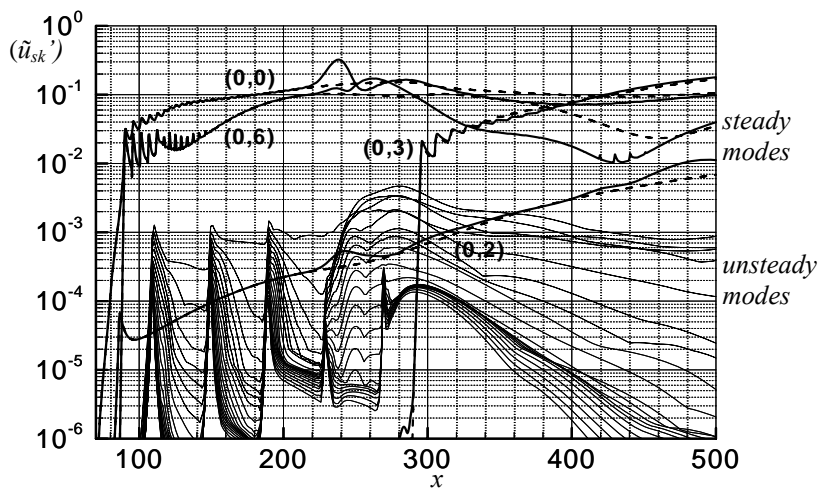


Figure 6. Amplitude development for DFD suction with two slot panels (cf. Fig. 5). Steady modes: (0,6) first DFD mode, (0,3) second DFD mode, dashed reference case Fig. 5a, solid for Fig. 5b. Unsteady modes: pulse disturbances ($\omega=0.225-4.5$, $\Delta\omega=0.225$, time-spectral) to check for secondary instability in case b), excited at five successive x -positions with $k=2$.

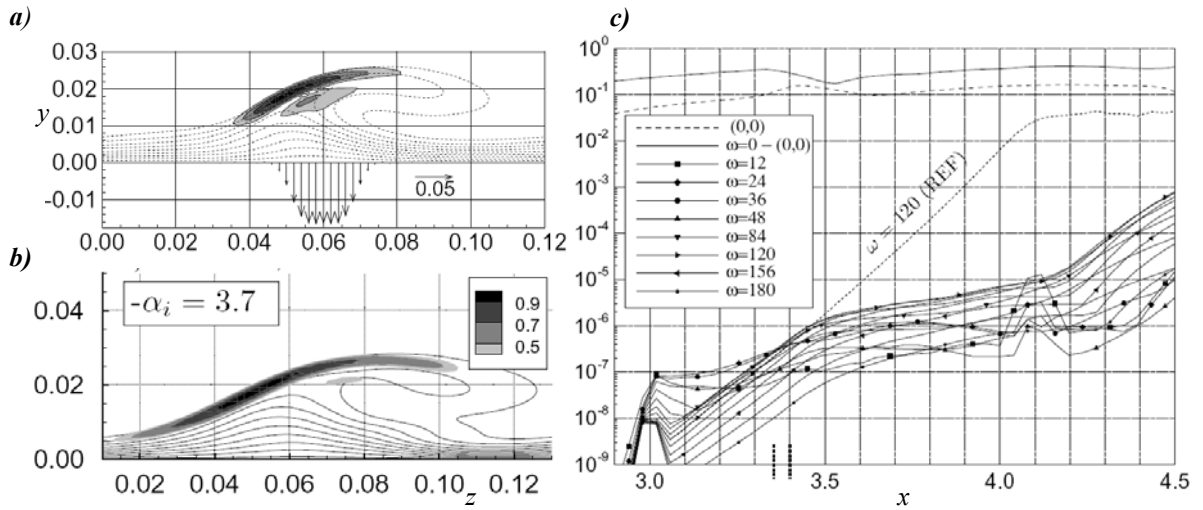


Figure 7. Setup and amplitude development for pinpoint suction.

- a) Flow crosscut at $x=3.38$ with amplitude distribution of secondary-instability mode $\omega=132$ (shaded) and u/u_e -velocity iso-contours for the vortex-deformed flow without suction; the arrows indicate the applied suction leading to figure b);
 b) Same as figure a) but at $x=3.84$ with suction at $x=3.38$.
 c) Modal amplitude (\tilde{u}_{sk}') development for the case with suction; REF: case without suction.

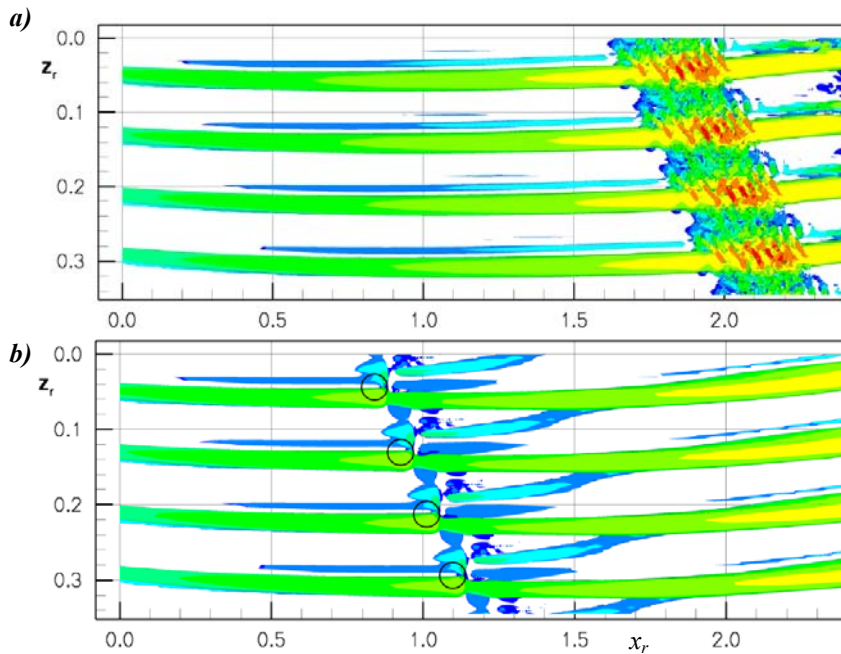


Figure 8. Visualization of vortex structures for pinpoint suction. Shown are λ_2 iso-contours (snapshot), the color indicating the wall-normal distance: blue for $y=0$, red $y=0.04$, and green and yellow intermediate. A rotated reference system has been used for visualization: $x_{r0}=2.79$, $z_{r0}=0.0$, $\Phi_r=45.86^\circ$. The domain covers approx $x_r \in [2.6, 4.3]$. Note the compression of the x_r axis; a) crossflow secondary-instability scenario without suction, b) with suction marked by the circles. Top view on plate, mean flow from left to right.

B. Results

An almost stagnating amplitude growth can be observed up to $x=4.1$ in Fig. 7c and transition is pushed out of the considered domain. The development of the type-I mode downstream of the suction reveals a stretching and weakening effect on the mode (Fig. 7b) leading to smaller amplitude growth and hence a longer laminar regime. With suction also the vortex itself is weakened as the suction applied at the updraft side inhibits its rotating motion. Fig. 8b reveals steady CFVs with a pair of steady, fading secondary longitudinal vortices close to the wall generated by the suction in between the primary CFVs. Suction through holes always generates a pair of counter-rotating longitudinal vortices where, with crossflow, only one of them survives. It is the one that transports fluid near the wall with the basic crossflow. In Fig. 8b this is the second longitudinal, light-blue structure above each primary, green CFV. This structure is pressed to the wall by the next, co-rotating primary CFV, and fades out somewhat later than its counter-rotating partner. For the reference case in Fig. 8a the pulses grown to traveling secondary finger-type vortices at the same time level can be seen. A case with blowing at similar position¹⁴, enhancing the vortex itself, also exhibits a weakening of secondary instability, albeit to a lesser extent. Suction through a spanwise slit, optimal for lowering primary crossflow instability, does not show notable secondary-growth attenuation¹⁴.

Further investigations show that misplaced blowing or suction holes can generate strong shear layers that may even enlarge the amplitude growth rates of secondary modes. A well-positioned hole pattern that is adapted to the local deformed-flow characteristics, especially the vortex situation, is therefore indispensable. More results for directly attacking secondary crossflow instability using pinpoint blowing or suction, including unsteady forcing, can be found in Ref. 14.

VI. Conclusions

The DNS results show that the combination of the Upstream-Flow-Deformation technique, where useful crossflow vortices are forced, can be advantageously combined with suction for laminar flow control in three-dimensional boundary layers on swept wings. The vortices, deliberately excited by an appropriate suction orifice order and amplified by instability, enhance the suction effect by their additional meanflow alteration, and a stabilization better than by ideal homogeneous suction can be achieved. Equivalently, the suction rate can be lowered for the same stabilization. For strongly varying baseflows Distributed-Flow-Deformation suction with excitation of successively subharmonic spanwise modes has been demonstrated to work, even in case of a steady baseflow disturbance by a local pressure rise. We point out that the useful vortices can also suppress disturbances other than the ones generated by the suction itself. It remains to be checked whether the DFD technique also works without net suction but with synthetic blowing or suction. It has also been demonstrated that it is possible to directly exert a significant weakening influence on highly unstable secondary-instability scenarios, up to complete stabilization, by accurately positioned, pinpoint suction with moderate suction rates. Thus spatially fixed vortices can be controlled.

Acknowledgments

The partial financial support by the Deutsche Forschungsgemeinschaft and Airbus Deutschland GmbH is gratefully acknowledged as well as the provision of supercomputing time by HLRS, Stuttgart, within project LAMTUR. I also acknowledge the invitation to come to the Seattle conference extended by Hermann Fasel, University of Arizona, Tucson, Az, in the year of his 65th birthday.

References

- ¹Wassermann, P. and Kloker, M., "Mechanisms and Passive Control of Crossflow-Vortex-Induced Transition in a Three-Dimensional Boundary Layer", *J. Fluid Mech.*, Vol. 456, 2002, pp. 49-84.
- ²Bertolotti, F.P., "The Equivalent Forcing Model for Receptivity Analysis with Application to the Construction of a High-Performance Skin Perforation Pattern for LFC", *Recent Results in Laminar-Turbulent Transition* edited by S. Wagner, M. Kloker, U. Rist, NNFM 86, Springer-Verlag, 2004, pp. 25-36.
- ³Messing, R. and Kloker, M., "DNS Study of Discrete Suction in a 3-D Boundary Layer", *Recent Results in Laminar-Turbulent Transition* edited by S. Wagner, M. Kloker, U. Rist, NNFM 86, Springer-Verlag, 2004, pp. 177-188.
- ⁴Messing, R. and Kloker, M., "Smart Suction - an Advanced Concept for Laminar Flow Control of Three-Dimensional Boundary Layers", *High Performance Computing on Vector Systems 2007* edited by M. Resch et al., Springer-Verlag, 2008, 8 pages.
- ⁵Saric, W., Reed, H.L., White, E.B., "Stability and Transition of Three-Dimensional Boundary Layers, *Annu. Rev Fluid Mech.*, Vol. 35, 2003, pp. 413-440.
- ⁶Bonfigli, G. and Kloker, M., "Secondary Instability of Crossflow Vortices: Validation of the Stability Theory by Direct Numerical Simulation", *J. Fluid Mech.*, Vol. 583, 2007, pp. 229-272.

- ⁷Friederich, T., "Active Control of the Crossflow Secondary Instability in a 3-d Boundary Layer Using Steady Blowing and Suction", Master Thesis, Institut für Aerodynamik und Gasdynamik, Universität Stuttgart, 2007.
- ⁸White, E.B., Saric, W.S., "Secondary Instability of Crossflow Vortices", *J. Fluid Mech.*, Vol. 525, 2005, pp.275-308.
- ⁹Koch, W., Bertolotti, F.P., Stolte, A. and Hein, S., "Nonlinear Equilibrium Solutions in a Three-Dimensional Boundary Layer and Their Secondary Instability", *J. Fluid Mech.*, Vol.406, 2000, pp.131-174.
- ¹⁰Wassermann, P. and Kloker, M., "Transition Mechanisms Induced by Traveling Crossflow Vortices in a Three-Dimensional Boundary Layer", *J. Fluid Mech.*, Vol. 483, 2003, pp. 67-89.
- ¹¹Spalart, P.R., "Numerical Study of Transition Induced by Suction Devices", *Proceedings of the Conference on Near-Wall Turbulent Flows* in Tempe, Florida, edited by R.M.C. So, C.G. Speziale, and B.E. Launder, Elsevier Science Publishers B.V., 1993, pp. 849-858.
- ¹²Joslin, R.D., "Aircraft Laminar Flow Control", *Annu. Rev. Fluid Mech.*, Vol. 30, 1998, pp. 1-29.
- ¹³<http://flight.tamu.edu/index.html>
- ¹⁴Friederich, T. and Kloker, M., "Localized Blowing and Suction for Direct Control of the Crossflow Secondary Instability" *AIAA-2008-4394*, AIAA Seattle Fluid Dynamics Conference, June 2008.